Nonlinear Time-History Seismic Assessment of 112-Year-Old Barossa Dam

Francisco Lopez and Michael McKay

GHD Pty Ltd, Melbourne

Abstract

At 36 m high and completed in 1902, Barossa Dam is one of the first true concrete arch dams in the world. During the 1954 Darlington Earthquake the dam sustained some damage, in the form of several vertical cracks on both dam's abutments. In 2013, GHD conducted a nonlinear time-history seismic assessment of Barossa Dam. The analyses, carried out using finite element techniques, included ground motion loading corresponding to Maximum Design Earthquakes (MDEs) with 1 in 10,000 Annual Exceedance Probability (AEP).

This paper will explain the purpose of the study, the material investigation phase, the methodology, model results, the anticipated seismic behaviour of the dam wall, as well as the predicted level of damage under the MDEs. The paper examines the dam construction practices of the beginning of the 20th century, and how such practices affected the material properties and the structural performance of Barossa Dam.

Keywords: *Arch, seismic, construction practices, nonlinear, damage prediction.*

Introduction

In order to capture the nonlinear behaviour, and to predict whether it can safely withstand Maximum Design Earthquakes (MDEs) with an Annual Exceedance Probability (AEP) of 1 in 10,000, a nonlinear time-history analysis of Barossa Dam was conducted by GHD. The description of the dam, a layout of the adopted methodology, a summary of the results and the conclusions of the assessment are presented and explained in this paper.

Typical arch dams may respond nonlinearly to earthquake loading, during which contraction joints could open and close repeatedly as the dam vibrates. Although Barossa Dam does not possess contraction joints, it does exhibit some vertical cracking (caused by an earthquake in 1954) which may resemble the behaviour of vertical contraction joints during seismic loading.

Crack opening during the earthquake may help release tensile arch stresses but it may also increase the compressive and tensile stress demand on the cantilevers. The redistribution of stresses may lead to concrete crushing, particularly at the toe of the dam and on the sides of the cracks, while the tensile strength of the lift joints may exceed generating cracking along these surfaces. High tensile stresses could also develop along the dam-foundation interface that may result in cracking along the dam-foundation contact or displacements and permanent deformations of the foundation rock.

Another form of nonlinear behaviour in arch dams is the potential transfer of sliding demand from an unstable monolith (or a section of a monolithic dam) adjacent monoliths (or sections) with 'spare' sliding strength.

Description of the dam wall

Barossa Dam, owned by the South Australian Water Corporation (SA Water) was constructed between 1899 and 1902 to supply domestic water to the township of Gawler. Later, in 1942, the supply was linked with the Adelaide metropolitan system.

The dam comprises a cylindrical concrete arch wall, which at the time of construction was the highest concrete arch dam in Australia and amongst the first true arch dams constructed in the world. A cross section indicating the dimensions and other details of the dam are presented in Figure 1.

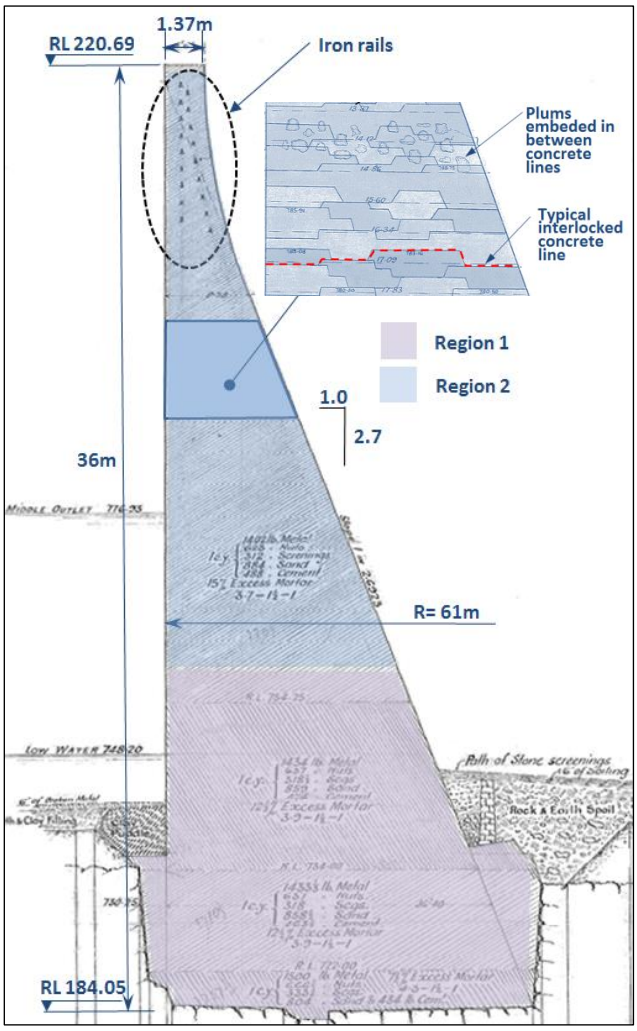

Figure 1: Barossa Dam - Details of maximum section

The crest is 36 m above the lowest foundation level and 1.37 m wide. The arch radius is 61 m, with a vertical upstream face. The downstream face has a constant slope of 1H: 2.7V down to foundation level.

Plums varying in size between 0.03 and 0.45 m^3 were used to economize on the use of mixed concrete, accounting for approximately 13% of the volume of the dam. A minimum of 150 mm of mixed concrete thoroughly rammed and worked with long-handled slicers was placed between adjacent plums. No plum placing was allowed in the top 4.6 m of the dam, within 0.5 m of the upstream face, or within 0.3 m of the downstream face. Each plum was well rammed with wooden malls to bed it into the concrete. In the top 4.2 m of the wall eighteen second-hand iron rails were placed as arch reinforcement.

Reflecting the design practices at the start of the 20th century, the wall does not present contraction joints. According to the historical account of Barossa Dam (EWS 1985), in reference to design of the dam to withstand thermal stress, *"it was decided somewhat arbitrarily that as the bottom of the dam was fixed in rock it should have enough 'spring' to accommodate this movement without cracking"*.

The current visual condition of the dam, inspected from on the crest and downstream side only, can be described as fair. Several significant near vertical cracks, most likely resulting from the 1954 Darlington Earthquake, are present on the dam wall (the most prominent being three on the left abutment and one on the right abutment), although they are dry and appear to be inactive. Generalised efflorescence, resulting mostly from leakage through horizontal concrete lifts, can be observed on the downstream face of the dam. There is also generalised micro cracking and some minor wet patches. There is no significant leakage or evident signs of distress on the dam wall when the reservoir is at Full Supply Level (FSL).

Seismic environment of the Barossa Dam area

Barossa Dam is located within the Mt Lofty Ranges in South Australia. The closest fault to the site is Williamstown Fault, located approximately 5 km away, which dips to the east away from the dam. The Para Fault, located approximately 10 km away, dips east and towards the dam site. Both faults are believed to be active, suggesting possible movement in recent geological time.

The 1954 Darlington Earthquake

According to the Department of Mines (1973), cracks on Barossa Dam were first noticed after the 1954 Darlington earthquake. The epicentre was located along the Eden Fault in the Darlington area, about 45 km south west of the dam site. Its duration at the dam site was about 10 seconds and the reported intensity was IV to V on the Modified Mercalli Scale. After the tremor up to 14 springs were reported on the right hand downstream bank of the gorge, but all dried up within a year. No other local effects were noticed in the reservoir area. The 1973 document also states that *"the sizes of the cracks have increased due to dissolution of cementitious material and they were more visible due to the deposition of calcareous material leached from the dam wall concrete"*.

Anecdotal reports indicate that the cracks appear to be continuous in the upstream-downstream direction, as they have been observed also in the upstream side at times of low reservoir levels.

Seismic hazard assessment of the Barossa Dam area

A specific seismic hazard assessment of the Barossa Dam area was conducted by others. The seismic hazard assessment included the development of response spectra for different periods of return and for 5% structural damping. The deaggregation plot for an event with 1 in 10,000 AEP and for a structural period of 0.2 s, indicated that the most damaging ground motions at the Barossa Dam site will be from earthquakes with magnitudes in the ML5.0 to ML7.5 range, and distances approximately 6 to 30 km from the dam site.

Time-history ground motions

Three sets of acceleration time-histories considered representative of the tectonic environment of Barossa Dam, for MDEs of 1 in 10,000 AEP, were also developed by others. Each set comprised three components, namely upstream / downstream, cross valley and vertical.

In the absence of specific strong motion data for Barossa Dam region, it was necessary to adjust 'foreign' time-history accelerograms imported from worldwide strong motion databases. The selected foreign time-histories were modified to be closer to the target spectrum (the 1 in 10,000 AEP spectrum developed for the Barossa Dam area) using the Simple Spectrum Scaling approach (USACE 2003). In the simple spectrum scaling method the same scaling factor is applied to all three components of the acceleration time-histories, preserving the relative amplitudes of the three different components of the same record.

The selected earthquakes used to generate the acceleration time-histories with 1 in 10,000 AEP for Barossa Dam are presented in Table 1.

Table 1: Selected Ground Motions

Earthquake	Station	Year	Ms	Distance (km)	PGA (m/s^2)
Tabas (Iran)	Dayhook	1978	7.4	11	4.6
Loma Prieta (California, USA)	Gilroy Array #1	1983	6.9	10.5	3.95
Coalinga (California, USA)	Oil Fields Fire Station Pad	1983	5.7	10.9	4.03

Also in accordance with a recommendation by USACE (2003), in order to avoid being unconservative at periods where the valleys of the time-history response spectrum are less than the target spectrum, a fit test for the three time-histories was performed. For the fit test, the mean of the dominant horizontal component of each of the three

sets of time histories was calculated period by period. As recommended by USACE, it was confirmed that the obtained mean spectrum was no less than 85% of the target response spectrum in the defined frequency range that is of significance to structural response (that is 1 to 20 Hz for concrete dams).

For illustrative purposes, the horizontal component with the larger acceleration spike on each of the generated time-histories is presented in Figure 2.

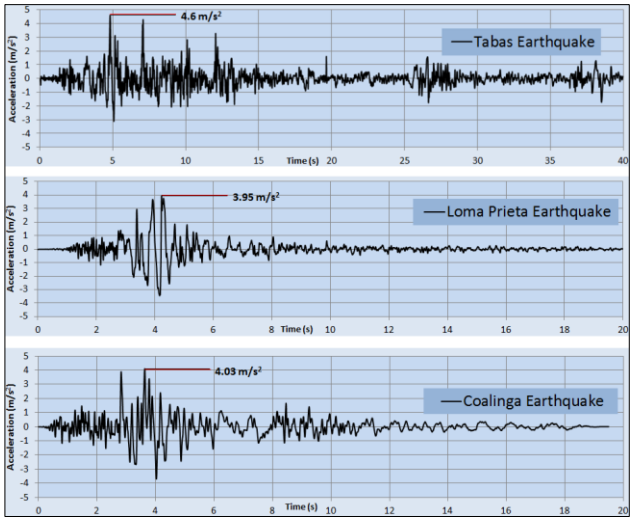

Figure 2: Acceleration time-histories (only most demanding horizontal component shown)

Seismic assessment of the dam

Factors of safety and adopted acceptance criteria

In general, the structural integrity of an arch dam is maintained and the dam is considered safe if it has acceptable factors of safety for the various failure modes such as overstressing and sliding. The Factors of Safety (FoS) for different failure modes presented in the guidelines for design of arch dams by USACE (1994) were adopted as the basis to define the acceptance criteria for this study.

Factors of safety are required in the assessment of dams because of uncertainties in the load and material parameters, as well as the assumptions or simplifications made in the analysis procedures and techniques. Both USACE (1994) and FERC (1999) state that the factors of safety may be altered using engineering judgement, based on the quality of the information available for a particular project. It is noted that in both documents the recommended FoS for tensile strength is 1.0.

In the case of Barossa Dam, a tensile strength FoS of just 1.0 seems inappropriate, as it leaves no margin for any uncertainty. Furthermore, there were no detailed construction records, and the estimation of the tensile strength of the concrete was based on only three direct tensile tests. Hence, it was deemed appropriate to increase the factors of safety for tensile stresses. However, since dam design guidelines do not suggests alternative factors of safety when the available information is scarce, a strength reduction factor was adopted to indirectly increase the factors of safety recommended by USACE.

The ACI Building Code (ACI 2008) states that one reason to use strength reduction factors is to allow for potential under-strength members due to variations in material strengths and dimensions. In plain (mass) concrete, since both flexural tension strength and shear strength depend on the tensile strength characteristics of the concrete (with no reserve strength or ductility possible due to the absence of reinforcement) equal strength reduction factors are appropriate for both bending and shear. ACI suggests a strength reduction factor of 0.6 for bending and shear, supported by reliability analyses and statistical studies of concrete properties as well as calibration against past practice. Based on a strength reduction factor (Φ) of 0.6 suggested by ACI for tensile strength in plain concrete, for this study the FoS for tensile strength were increased to 1.7 (i.e. 1.0/ 0.6).

The acceptance criteria adopted for the seismic assessment of Barossa Dam, based mainly on USACE (1994) and including a modification to the FoS for tensile strength, are presented in Table 2.

Table 2: Adopted acceptance criteria for Barossa Dam

Load condition	Factors of Safety for:		
	Compressive Stress	Tensile Stress 1	Sliding Stability
Static			
Usual	4	1.7	2
Unusual	2.5	1.7	1.3
Extreme	1.5	1.7	1.1
Dynamic			
Unusual	2.5	1.7	1.3
Extreme	1.5	1.7	1.1

Material properties

Foundation rock

In general the foundation rock consists of interbedded quartzitic sandstone and siltstone, with occasional bands of quartzite. The bedding dips approximately 37° towards the right abutment of the dam. There is an observed weathering profile with depths ranging from 5 to 10 m. The description of the identified rock zones is presented Table 3.

Table 3: Identifications of the foundation rock zones

Zone	Rock Type	Location	Strength	Rock Modulus
1	Quartzite/ Sandstone	Top 3 m right abutment	Low	-
2	Quartzite/ Sandstone	Weathered, top 5 to 10 m of rock across the valley. Removed during excavation for the dam	High	6.2 GPa
3	Quartzite/ Sandstone	Moderately weathered rock on upper half of right abutment	High	8.8 GPa
4	Quartzite/ Sandstone	Strong rock	Very High	18 GPa
5	Quartzite/ Sandstone	Sandy clay crushed seam dipping sub-parallel to left abutment		-

For practicality, non-relevant rock zones were not accounted for in the Finite Element (FE) model of Barossa Dam. Zone 1 was disregarded because it is relatively shallow, is above the base of the concrete and is limited to a small zone on the top of the right abutment. It does not affect the overall deformation of the dam or the foundation. The crushed seam (Zone 5) was also ignored in the FE analysis since the deformation modulus of the surrounding rock mass of Zone 4 accounts for the presence of defects such as discontinuities, faults, joints, etc. The crushed seam, however, plays an important role as it may define a potential instable rock wedge that was also assessed during the project, but is not part of the present paper.

The excavation of the dam was taken down to the level of the less weathered, more competent rock.

Parent concrete

Barossa Dam documents show that different concrete mixes were used over the height of the dam. For the purpose of the structural analysis of the dam, simplification was made of the various concrete mixes and they have been grouped into two regions in the wall: Region 1 in the bottom 13 m, and Region 2 on the top 23 m (refer to Figure 1).

During the investigation phase concrete cores were extracted from the wall at three locations. The cores were tested for evaluation of the compressive strength, direct tensile strength, modulus of elasticity and Poisson ratio. Whilst the concrete coring intercepted horizontal lift joints in the dam, no intact joint specimens were recovered and hence the tests were performed on parent concrete only. The adopted material properties for parent concrete are presented in Table 4.

Table 4: Adopted material properties for parent concrete

Property	Region 1	Region 2
Density (kg/m^3)	2,200	2,200
Compressive strength - Static (MPa)	40.5	50
Compressive strength - Dynamic (MPa)	52.7	65
Tensile strength - Static (MPa)	1.5	2.3
Tensile strength - Dynamic (MPa)	2	3
Modulus of elasticity - Dynamic (MPa)	14,000	14,000
Modulus of elasticity - Static (MPa)	14,000	14,000
Poisson's ratio - Static	0.15	0.15
Poisson's ratio - Dynamic	0.15	0.15
Tensile strength vertical cracks (MPa)	0	0
Shear modulus vertical cracks (MPa)	3,500	3,500

For the dynamic cases an increase in the strength of the concrete is expected due to the rapid rate of the application of the seismic loading. Both the dynamic compressive and tensile strengths were estimated 30% larger than the static ones (USBR 2006).

It was also assumed that there is no tensile strength across the near vertical cracks on the abutments of the dam. However, it is expected that the cracks, which are apparently no wider than 5 mm and seem inactive, retain some shear stiffness due to the interlocking effect of the aggregate on the faces of the cracks.

Concrete lift joints

One of the major sources of uncertainty in the analysis of concrete dams is the condition and strength of the lift joints compared to the parent concrete. The shear and tensile strength of bonded lift joints depend on various factors but are generally less than for parent concrete and thus constitute the weak points in the dam wall. Even though some joints may be unbonded, they could have some shear strength. Partially and fully unbonded lift joints have no tensile strength in the unbonded areas, which may affect the overall damping and modulus of elasticity of the dam wall.

Unbonded lift joints can be detected by examination of drilled cores and by direct observation of leaking joints on the downstream side of the dam. However, coring is usually limited to certain locations of the dam within reach, and therefore the results may not be representative of the whole structure. The determination of the condition of the lift joints and the overall strength of the dam based on limited available testing remains a challenge for dam engineers.

Dolen (2011) presents ratios of bonded to unbonded lift joints for dams of different ages. In the construction period of interest (1905 to 1933, with Barossa Dam constructed in 1899 to 1902) the average number of bonded joints is 50%, with individual data ranging from 9% to 83%. He noted that one factor affecting the lift joint bond strength of these old dams was the practice of placing overly wet mixtures with excessive bleeding and laitance. This practice was the consequence of additional water being added to transport concrete in long chutes and to consolidate the mass concrete in higher lifts. Dolen states that the introduction of the highline bucket method for placing mass concrete (circa 1930) and the internal mass concrete vibrator (circa 1934) allowed placing lower slump concrete, with a subsequent improvement in the lift joint properties. This seemed to be confirmed by the results of the average of bonded lift joints in the period 1933 to 1964, which improved to 85%.

In regards to the construction practices and a potential improvement to the lift joint bond strength, Barossa Dam may have been ahead of its time. The historical account of the dam (EWS 1985) indicates that *"…the wet mix was placed in a skip and taken to the pouring site by flying fox"*. This is similar to the highline bucket technique that according to Dolen was not introduced in the USBR dams until 1930. It is also clear that the people in charge of the design and construction of Barossa Dam were well aware of the importance of a proper bond strength between lift joints, as inferred from this fragment of the historical account: "*… placing of concrete was carried out in continuous horizontal layers 230 mm thick and much care was taken to ensure efficient bonding between layers. Each layer was well chopped with iron bars or blunt-ended swords and thoroughly punned with wooden rammers…"*. EWS (1985) also indicates states that concrete was placed in continuous horizontal layers of 230 mm thickness. Historical drawings and photos of the

construction of Barossa Dam also show that the concrete lifts were discontinuous, had variable thickness, and form shear keys (refer lift details on Figure 1) that contribute to the overall shear strength of the dam.

Based on the average percentages of bonded joints reported by Dolen in the earliest period reported (50% in 1905 to 1933), the average percentage of bonded joints in the period with construction practices similar to those used at Barossa Dam (85% in 1933-1964), and after the direct observation of leaking and efflorescence on the downstream face of the dam, the adopted percentage of bonded joints in Barossa Dam was 70%.

In terms of historical tensile strength, for dams constructed in the period 1905 to 1933, Dolen provides data with an average ratio of bonded lifts strength to parent concrete strength of 45%. This ratio was used to estimate the tensile strength of the concrete lifts of Barossa Dam. The unbonded lift joints, as previously stated, are assumed to have nil tensile strength.

A practical approach to adopt a global lift joint strength for the dam, as proposed by Dolen, consists of reducing the average values by the estimated fraction of bonded lift joints, i.e. 70% in the case of Barossa Dam. The estimated global lift joint strengths for this study, combining bonded and unbonded joints, are presented in Table 5. For example, the dynamic direct tensile strength for Region 2 is 0.9 MPa, calculated as 3.0 MPa (strength of parent concrete, refer to Table 4) x 0.45 (ratio bonded lift to parent strength) x 0.7 (percentage of bonded lifts).

Table 5: Adopted material properties for lift joints

Property	Region 1	Region 2
Tensile strength - Static (MPa)	0.5	0.7
Tensile strength - Dynamic (MPa)	0.65	0.9
Shear strength	Discussed in the "Radial sliding" section	

Finite Element (FE) model

Barossa Dam was modelled and analysed using the program DIANA. The FE model of Barossa Dam included the reservoir, the dam and its vertical cracks, the three different identified rock zones in the foundation, and the dam-foundation interface (refer to Figure 3).

The 3-D finite element model of Barossa Dam was composed of 85,469 solid Tetra-type elements representing the dam wall and the foundation, 4,903 fluid elements representing the reservoir, and 1,289 interface elements representing the contacts between the dam and the foundation and the vertical cracks of the dam. The extent of the foundation in the model was determined as a function of the height and cross valley dimension of the dam, as recommended by USBR (2006).

Figure 4 (with Zone 2 rock hidden) shows the relative size of the finite elements of the model and the nonlinear interfaces. The crack interfaces within the dam body represent the three near vertical cracks on the left abutment and the one on the right abutment. The dam-foundation interface extends along the full contact between the dam and the foundation.

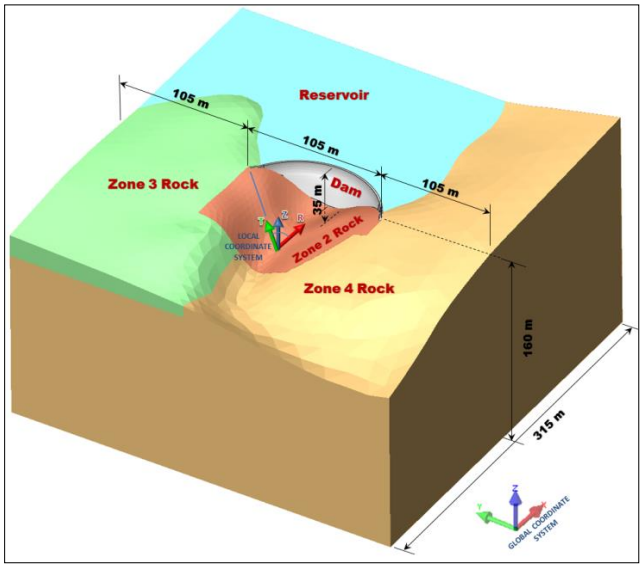

Figure 3: Rendered FE model of Barossa Dam

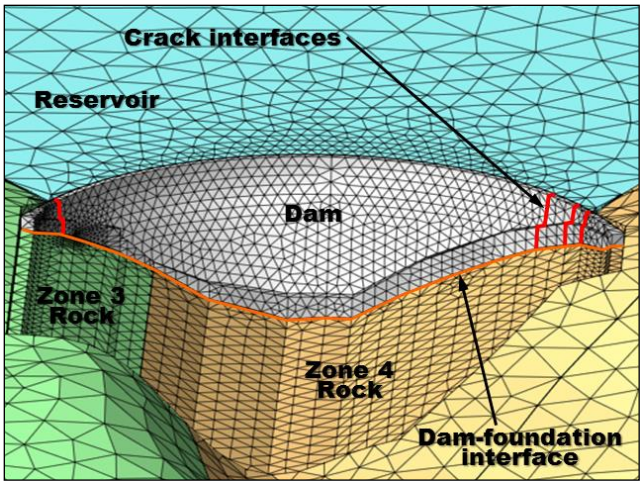

Figure 4: Nonlinear contacts in FE model

Nonlinearity of the model

The model developed for Barossa Dam is capable of reproducing the typical nonlinear behaviour of arch dams, as explained in the Introduction of the paper. In a phased approach, the initial nonlinearity of the model was restricted to geometrical nonlinearity only (i.e. at interface surfaces and discontinuities), with all structural materials responding to linear-elastic constitutive models. Material nonlinearity in the form of 'smeared crack' concrete material or Mohr-Coulomb rock material would be used in a further phase of the study only if the results of the initial phase were inconclusive.

The geometrical nonlinearity was introduced in the model using Coulomb-Friction and Discrete Crack element type, as described below. The normal and shear stiffness for each contact element are presented in Table 6.

Coulomb-friction elements were used to model the dam-foundation interfaces (at the dam base and at the contact between the dam and the upstream and downstream faces of the excavation). This type of interface allows opening and closing of the discontinuity and can provide tensile strength up to a specified value. It also models the friction force that exists between two dry contact surfaces.

The Coulomb-friction interface requires the definition of the initial stiffness modulus (normal, k_n, and shear, k_t). The stiffness moduli of the interface should be larger than the stiffness of the two materials in contact to prevent over-penetration (i.e. dam base protruding into the foundation rock). These values are therefore determined by calibration of the model. Other variables required for this element are the cohesion and angle of friction of the modelled surface, which were adopted based on the assessed conditions of the dam-foundation interface.

Table 6: Adopted normal and shear stiffness

Location	Type	Normal Stiffness Modulus k_n (MPa/m)	Shear Stiffness Modulus k_t (MPa/m)
Dam-foundation interface (base-centre of valley)	Coulomb-friction	$6.5x10^6$	$6.5x10^6$
Dam-foundation interface (base of abutments)	Coulomb-friction	65,000	6,500
Dam-foundation Interface (upstream and downstream faces of excavation)	Coulomb-friction	$6.5x10^6$	6,500
Dam crack interface elements	Discrete	$6.5x10^6$	$6.5x10^6$

Discrete-cracking elements were used to model the near vertical cracks on the abutments of the dam and the presence of iron rails crossing the cracks in the dam crest region. This type of interface allows opening and closing of the discontinuity, can provide tensile strength up to a specified value and allows shear retention due to interlocking of aggregate on the faces of the cracks.

The discrete-crack elements on the vertical cracks respond in a brittle manner, with full reduction of the strength and opening of the crack width after the tensile capacity (tension cut-off) has been reached. In the area where the rails cross the cracks, a tension cut-off of 0.6 MPa was estimated as the tensile force provided by the iron rails, divided by the gross area where the rails are located (7 m^2). The tensile force of the rails was estimated as the combined cross-sectional rail area (0.04 m^2) multiplied by the typical minimum tensile strength of the rails around the time of construction of Barossa Dam. Since the characteristics of the rails are unknown a conservative tensile strength of 105 MPa was adopted, corresponding to a typical value for cast iron in the mid-1800s.

The discrete-crack interface also requires the definition of normal and shear stiffness. The shear retention in the cracked area without rails (1,400 MPa/m) was estimated as 25% of the modulus of elasticity of uncracked concrete, divided by the average element size (2.5 m). The shear retention in the crest area with crossing rails (1,600 MPa/m) was calculated as the weighted average of the shear retention of cracked concrete and the shear modulus of iron, divided by the average element size.

Loads

A description of the loads acting on the dam-reservoir-foundation system, and how they were accounted for in the model, is presented below.

- Structure self-weight: Based on the dimension and density of the materials. For the seismic cases, the foundation was considered massless.
- Hydrostatic forces from reservoir: Applied as pressure normal to the upstream face of the dam wall and to the bottom of the reservoir, for the water at Full Supply Level (FSL), that is, 0.6 m below crest level.
- Uplift: Applied as an internal pressure at the interface between the dam and the foundation rock, following a preliminary steady-state flow analysis that established the stress field of the dam-foundation system (refer to McKay and Lopez 2013). The prescribed uplift pressure profile varies linearly from full reservoir water head on the upstream side to full tailwater level on the downstream side. At locations where cracking of the dam-foundation interface was predicted under static loading, it was assumed that the full length of the crack is pressurised to the full reservoir water head. The uplift pressure was assumed to remain unaltered during the earthquake. However, it was adjusted for the post-earthquake analysis in accordance with the predicted earthquake damage on the wall.
- Pore pressure: Applied as an internal pressure in the dam's body, following a preliminary steady-state flow analysis that established the stress field of the dam-foundation system under static loading (refer to McKay and Lopez 2013).
- Earthquake: Applied on the external boundaries of the FE model in the form of acceleration-time histories with an AEP of 1 in 10,000. The hydrodynamic effect of the reservoir was accounted for using fluid elements and hydrodynamic masses (separately).
- Temperature: Not included. In the case of existing dams where the closing temperatures are unknown, as is the case of Barossa Dam, the closing temperature (stress free temperature) can be assumed to be approximately the annual mean temperature. For the Barossa Dam area the difference between average and minimum annual temperatures are relatively small and has only very minor impact on the calculated stresses in the dam.

Foundation mass

Unless modelled as an almost infinite long and deep field, foundations with mass and finite boundaries will alter the response as it traps seismic energy and reflects it back into the dam. A massless foundation, which is commonly used in the finite element analysis of dams, is not entirely realistic, but eliminates this problem by removing the inertia from the foundation, while maintaining its stiffness. The use of a massless foundation, however, ignores the radiation damping component, therefore could

lead to more conservative stresses and displacements in the dam.

Alternatively, infinite non-reflecting boundaries at the outer edges of the foundation could be used, the most common one called Lysmer-Kuhlemeyer boundary. The non-reflective boundaries represent the energy absorption of incident S and P waves. However, unless properly calibrated, these boundaries may overestimate the damping of the system and lead to unconservative values. More recently (Basu 2008) proposed the Perfectly Matched Layer (PML) model, a rigorous mathematical solution to the problem that is still to be implemented in commercial FE packages.

For the reasons explained above it was deemed appropriate for this study to adopt the more conservative massless foundation approach for the earthquake analysis of Barossa Dam.

Strength assessment methodology

The stress assessment for Barossa Dam consisted of comparing the resulting compressive and tensile stresses in the dam against the allowable stresses for concrete. The allowable concrete strengths were calculated as the strengths (presented in Tables 4 and 5), divided by the adopted FoS (presented in Table 2). For example, the net dynamic tensile strength for parent concrete in Region 2 of the dam is 3.0 MPa; the adopted FoS for tensile strength is 1.7; therefore the allowable tensile strength for earthquake cases is 3.0 MPa/ 1.7 = 1.8 MPa.

The stresses in the arch wall were assessed as follows:

- The vertical stress was compared with the allowable tensile strength of the concrete lift joints to assess the potential for de-bonding and crack advance on lift lines.
- The arch and principal tensile stresses were compared with the allowable tensile strength of parent concrete, to assess the potential for formation of vertical cracks (due to the arch stress) or in any other direction (due to principal stress).
- The principal compressive stress was compared with the allowable compressive strength to assess the potential for concrete crushing.

The magnitude, location and frequency of overstress excursions were also used to determine the expected damage in the dam and the foundation for the post-earthquake evaluation.

Stability assessment methodology

Since Barossa Dam has no vertical contraction joints, and hence no individual monoliths, the stability of the dam was conducted individually on 14 sections of the dam footprint. Figure 5 presents the sections in which the dam base footprint was subdivided into for the sliding assessment.

Sections 1, 2 and 3 correspond to blocks defined by the existing vertical cracks on the left abutment, while Section 14 corresponds to a block defined by the vertical crack on the right abutment. The arch wall was assessed for sliding along the dam-foundation contact zone in both the radial and arch directions

Radial sliding

Each section was assessed independently as a freestanding block, even though there are no independent monoliths or blocks in the dam other than those defined by the near vertical cracks on the abutments. Any deficit of restoring force on a given section was redistributed to neighbouring section, whenever the latter had enough redundancy to receive the transferred deficit.

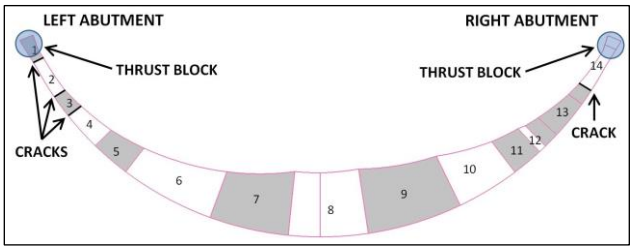

Figure 5: Dam base sections for sliding assessment

Radial sliding was assessed at the most critical of the potential failure surfaces at the dam-foundation interface zone: along the concrete-rock contact, along the first concrete lifts (particularly if they are unbonded), and along jointing and defects in the first 2 to 3 m below the dam base where the rock may have been disturbed during excavation. The following considerations on the shear strength were accounted for before selecting the critical surface for the sliding analysis:

- No specific shear strength tests were conducted at the concrete-rock contact in Barossa Dam. EPRI (1992) presents lower bound envelopes of shear strength for concrete in contact with different type of foundation rocks. For sandstones it shows an angle of friction of 65° and a cohesion of 345 kPa. However, lower angle of friction values are shown for other competent foundation materials, e.g. 53° for granite.
- EPRI (1992) also presents lower bound envelopes of shear strength for concrete lifts: an angle of friction of 57° and a cohesion of 965 kPa for bonded joints, and an angle of friction of 48° and no cohesion for unbonded joints. Since a combination of bonded and unbonded conditions is expected, the same principle of strength proportionality between bonded and unbonded joints (explained in the "Material properties" section of this paper) was used to estimate the shear strength parameters for the concrete lifts. With an estimated 70% of bonded joints, the adopted shear friction properties for the concrete lifts were an angle of friction of 54° and a cohesion of 345 kPa.
- Along the jointing and defects in the first 2 to 3 m below the dam base, and estimation of the shear strength using the Hoek-Brown (1980) criteria resulted in an angle of friction of 55°. No cohesion was assumed, although it is clear that bridging between jointed block needs to occur to form this failure surface.
- Based on the previous considerations, a conservative approach was adopted for the definition of the shear strength properties of the dam-foundation interface. For

the sliding analysis an angle of friction of 53°, corresponding to the minimum value reported by EPRI for competent foundation rock, was adopted. Although some cohesion may also exist at the concrete-rock interface, no testing was conducted at Barossa Dam to accurately determine its value. Overestimation of the cohesion by minimal amounts may result in overestimation of the actual factors of safety. Therefore for the sliding analysis the cohesion at this interface was assumed to be zero.

In arch dams with significant excavation depths, as is the case for Barossa Dam (refer to the Foundation rock section in this paper), the downstream rock in contact with the toe of the dam is expected to contribute to the restoring forces, since such rock blocks would need to be mobilised before the dam can displace in the radial direction. Consequently, the radial sliding stability analysis can be reduced to the simple determination of the Sliding Safety Factor (SSF) of the passive downstream rock wedge, as shown schematically in Figure 6.

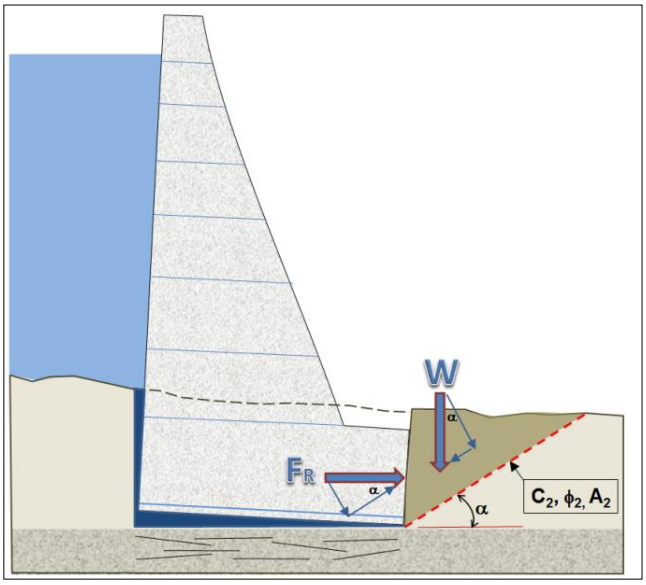

Figure 6: Radial sliding assessment

The radial sliding factor of safety (SSF) of the different sections is given by the relationship:

$$SSF_R = \frac{(W\cos\alpha + F_R \sin\alpha)\tan\phi_2 + C_2 A_2 + W\sin\alpha}{F_R \cos\alpha} \quad \text{(Equation 1)}$$

where F_R= resultant forces from FE model in the radial direction; W= weight of the downstream rock wedge; A_2, c_2, ϕ_2= shear area, cohesion and angle of friction, respectively, on downstream rock; and α= 45°- (ϕ_2 / 2).

Arch (tangential) sliding

As for the radial sliding, all 14 sections were assessed independently for sliding in the arch direction as freestanding blocks. Any deficit of restoring force on a given section was redistributed to neighbouring sections, whenever the latter have enough redundancy to receive the transferred deficit. Eventually, the excess of thrust force that cannot be resisted by the frictional capacity of the dam-foundation interface would be transferred to the wider thrusts blocks at the dam ends. For the dam not to slide in the arch direction, the forces transferred from the thrust blocks have to be resisted by the surrounding rock.

Arch sliding was assessed at the identified weakest plane at the dam-foundation interface, as shown schematically in Figure 7. Potential failure planes for arch sliding at the interface may occur by shearing across concrete (dashed blue line), shearing across the stepped excavation on Rock Zones 3 and 4 (red dashed line) or by shearing through defects in the foundation (green dashed line). In the case of Barossa dam the identified defects are Set A (bedding) and Set C (jointing).

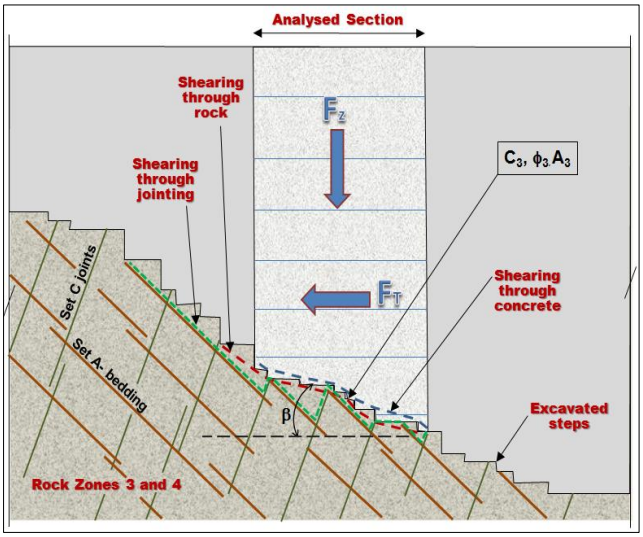

Figure 7: Arch (tangential) sliding assessment

A careful comparison of the potential shear strength of these failure planes indicated that shearing through bedding and jointing of the foundation was the critical arch sliding mechanism, for which frictional parameters of ϕ_3= 55° and c_3= 150 kPa were adopted.

The overall arch sliding stability of the different sections is given by the relationship:

$$SSF_A = \frac{F_Z \tan(\phi_3 + \beta) + \left(\frac{C_3 A_3}{\cos\beta\,(1 - \tan\phi_3 \tan\beta)}\right)}{F_T} \quad \text{(Equation 2)}$$

where F_Z= resultant forces from FE model in the vertical direction; F_T= resultant forces from FE model in the arch direction; A_3, c_3, ϕ_3= shear area, cohesion and angle of friction, respectively, on bedding/jointing sets; and β= abutment slope in the section being analysed.

Results of the assessment

The results of the seismic FE analysis of Barossa Dam, in terms of displacement, forces and stresses were examined to determine the expected level of damage on the wall. In this paper the stress and force (stability) results are presented in detail.

Stress on Dam

In terms of stress demand, the Loma Prieta Earthquake was the most critical. The summary of stress results for this earthquake is presented in Table 7.

Table 7: Stress result summary – Loma Prieta Earthquake

Parameter	Region 1	Region 2
Vertical Tensile Stresses (MPa)		
Maximum stress	2.0	1.5
Allowable stress (lift joint)	0.4	0.5
Assessment	Overstressed	Overstressed
Arch Tensile Stresses (MPa)		
Maximum stress	0.4	3.0
Allowable stress (parent)	1.2	1.8
Assessment	Pass	Overstressed
Principal Compressive Stresses (MPa)		
Maximum stress	3.2	3
Allowable stress (parent)	35.1	43.3
Assessment	Pass	Pass

A cross section with an envelope of maximum vertical stress at the tallest section of the dam is presented in Figure 8, in which the potential cracked and uncracked areas are identified by comparison of the acting vertical stresses against the allowable concrete lift strength. The expected level of overstress has the potential to develop continuous cracks along the lift joints from the upstream to downstream faces.

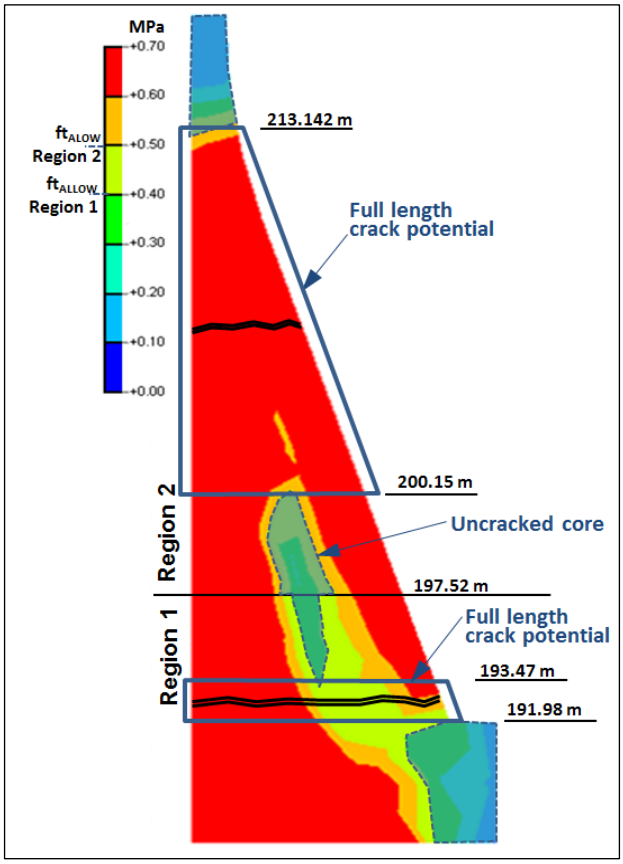

Figure 8: Vertical stresses – Loma Prieta Earthquake

The maximum arch stresses are located at the centre of the dam's crest, with overstress occurring on the top 4 m of the dam. Consequently, the development of one or a series of vertical cracks in this area is considered plausible. The maximum arch stresses on the existing vertical crack locations (0.58 MPa) was less than the adopted tensile capacity of the crossing iron rails (0.6 MPa). This stress assessment, along with the limited gap opening observed across the cracks, and the results of a previous sensitivity run without rails, indicates that the embedded rails play a key role in maintaining closure of the existing cracks during the MDEs.

Based on the stress results, it is anticipated that generalised cracking will occur in Barossa Dam as a consequence of MDEs with 1 in 10,000 AEP, with the potential of a freestanding block around 15 m wide and 7 m tall forming at the centre of the crest (refer Figure 9).

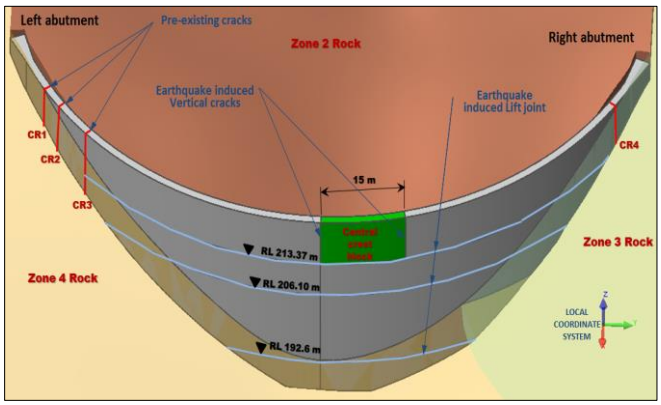

Figure 9: Expected cracking on dam wall after MDEs

A post-earthquake examination, considering the earthquake damage on the wall, with the reservoir maintained at FSL, was subsequently conducted. The dam as a whole, and also the individual cracked blocks (the existing ones on the abutments before the earthquake and the one generated on the crest), all satisfied the minimum FoS adopted for this study.

Stability assessment

The most demanding radial condition occurs for the Loma Prieta earthquake, for which the lowest sliding FoS was 1.04 at Section 9, but only at one single time step, with all other time steps above the minimum required sliding FoS of 1.1.

The arch stability plots indicate that the most demanding arch condition occurs for the Coalinga earthquake, for which the lowest FoS of 2.5 at Section 8 was obtained. The FoS for all other sections was more than the adopted minimum sliding FoS of 1.1, for the whole duration of the three earthquakes.

Based on the results instability of the dam in either the radial or arch direction is not expected. The acting shearing forces on the rock immediately downstream (which provides shear strength to the dam) is not large enough to shear it or to induce permanent downstream displacements on the dam.

Predicted damage in the dam wall

The results of the present assessment for displacement, stress and stability of the dam were used, along with engineering judgement and the review of available literature, to anticipate the damage to the wall of Barossa Dam as a consequence of the occurrence of MDEs with 1 in 10,000 AEP.

Damage due to displacements of the wall

The resulting vertical displacements at the dam-foundation interface are relatively small and are not indicating concurrent base detachment at both the upstream and downstream ends during the earthquake. However, both ends do detach from the foundation at different times, which indicates that there is potential for a full a crack to develop from upstream to downstream faces, with an increment of uplift pressure and leakage through the base as a result. This is even more likely due to the absence of drains at the foundation of Barossa Dam.

The differential movement on the sides of the existing near vertical cracks were very small, indicating little chance of grinding or a reduction of the shear strength of the cracks. This result suggests that the embedded iron rails play a key role in the seismic behaviour of the cracked blocks.

Crushing of concrete in the dam could result from the opening and closing of the existing vertical cracks and from partial lift-off at the toe and heel of Barossa Dam generated during the earthquake. Based on the relative small amplitude of the crack gaps obtained in this analysis, the likelihood of this type of damage is considered very small.

Some leakage through the existing cracks and cracks caused by the MDE could also be expected.

Damage due to overstress of concrete

USACE (2007) indicates that arch dams under seismic loading would typically exhibit high tensile stresses in the arch direction (in the upper part of the dam), and in the vertical direction (at the base of cantilevers). The results of the present nonlinear time-history stress analysis of Barossa Dam are consistent with these observations.

Based on the results of failed physical models of arch dams in a shaking table tests, Payne (2002) observed that the main failure mode for monolithic dam models, like Barossa Dam, initiated with a vertical crack that formed at the arch centre and extended two-thirds of the dam height downward from the dam crest. The results of this study coincide with that observation, although probably due to the limited amplitude of the used MDEs, estimated vertical crack on Barossa Dam is not expected to extend more than 5 m from the crest.

Damage due to sliding instability

There is no expected damage on the dam or the dam foundation interface since there is no predicted sliding displacements of the dam or shearing of the downstream rock wedge during the MDEs.

Conclusions

The present study indicates that under MDEs with 1 in 10,000 AEP Barossa Dam would be subjected to generalised overstress and potential cracking. Sliding failure of the whole dam or the existing cracked blocks is unlikely.

Most of the damage on the wall will consist of horizontal cracks due to excessive vertical stress across the lift joints. Superficial cracks would form on the lower two thirds of the dam, on both the upstream and downstream faces, and concentrated around the centre of the valley. However, there is also potential for horizontal lift cracks to form and propagate continuously from upstream to downstream faces.

In the central part of the crest there is potential for vertical cracks to form and meet the horizontal cracks, with the possible consequence of forming a freestanding block. This cracked block, however, would be linked to the dam by the embedded rails at crest level, which are not expected to fracture as a consequence of the earthquake.

Cracking along the full base of the dam-foundation interface could occur, particularly at the centre of the valley. Although the base lift-off does not occur simultaneously on the upstream and downstream ends, it is likely that continuous cracking from heel to toe will appear, creating a potential path for leakage through the interface.

Overall, Barossa Dam satisfies relevant dam design criteria for the MDE conditions. The dam is expected to suffer significant damage during the earthquake, but it is not expected to fail catastrophically during the event, or afterwards when the dam is subject to the normal load conditions. The expected level of damage would require extensive repair works and, most likely, the dewatering of the reservoir.

Acknowledgements

The authors would like express their thanks to:

- The South Australian Water Corporation (SA Water), owner of Barossa Dam, for permitting the publication of this paper.
- Professor Anil Chopra (UC Berkeley), for his technical advice and internal review of the seismic analysis of Barossa Dam.
- Mr Graeme Bell, for his technical peer review of the Barossa Dam project, and of this paper.
- Mr Derek Moore (SA Water) for his review of this paper.

References

ACI. 2008. *Building Code Requirements for Structural Concrete (ACI 318M-08) and Commentary*. American Concrete Institute.

Basu, U. 2008. Explicit finite element perfectly matched layer for transient three-dimensional elastic waves. *International Journal for Numerical Methods in Engineering 77*: 151-176.

Department of Mines of South Australia. 1973. *Geological Investigation Barossa*. *Sec. 1 Hd. Barossa*. Department of Mines South Australia, J. Selby, 14 November 1973.

Dolen, T.P. 2011. Selecting Strength Input Parameters for Structural Analysis of Aging Concrete Dams. *Proceedings of the 31st USSD Annual Conference*, San Diego, USA.

EPRI 1992. *Uplift Pressures, Shear Strength and Tensile Strengths for Stability Analysis of Concrete Gravity Dams*, Volume 1, USA.

EWS. 1985. *Barossa Dam – Historical Account of Construction and Operations*. The Engineering & Water Supply Department South Australia, Library Ref. No. 85/34.

FERC 1999. Chapter 11 - Arch Dams. *Engineering Guidelines for the Evaluation of Hydropower Project*, Federal Energy Regulatory Commission, USA.

Hoek, E. and Brown, E.T. 1980. Empirical Strength Criterion for Rock Masses, *Journal of Geotechnical Engineering*, ASCE 106 (GT9), 1013-1035.

Lopez, F. and McKay, M. (2013). Practical Methodology for Inclusion of Uplift and Pore Pressures in Analysis of Concrete Dams. *Proceedings of NZSOLD - ANCOLD 2013 Conference*, Rotorua, New Zealand.

Payne, T.L. 2002. Shaking Table Study to Investigate Failure Modes of Arch Dams. *Proceedings, 12th European Conference on Earthquake Engineering*, London, U.K., paper 145.

USACE. 1994. *Arch Dam Design, Engineering Manual EM 1110-2-2201*. US Army Corps of Engineers.

USACE. 2003. *Engineering Manual for Time-History Dynamic Analysis of Hydraulic Structures, Engineering Manual EM 1110-2-6051*. US Army Corps of Engineers.

USACE. 2007. *Earthquake Design and Evaluation of Concrete Hydraulic Structures Engineering Manual EM 1110-2-6053*. US Army Corps of Engineers.

USBR. 2006. *State of Practice for the Nonlinear Analysis of Concrete Dams at the Bureau of Reclamation*. U.S. Department of the Interior Bureau of Reclamation.